



Regional patterns of radiocarbon and fossil fuel-derived CO₂ in surface air across North America

Diana Y. Hsueh,¹ Nir Y. Krakauer,² James T. Randerson,¹ Xiaomei Xu,¹ Susan E. Trumbore,¹ and John R. Southon¹

Received 31 May 2006; revised 26 November 2006; accepted 11 December 2006; published 23 January 2007.

[1] Radiocarbon levels in annual plants provide a means to map out regional and continental-scale fossil fuel plumes in surface air. We collected corn (*Zea mays*) across North America during the summer of 2004. Plants from mountain regions of western North America showed the smallest influence of fossil fuel-derived CO₂ with a mean $\Delta^{14}\text{C}$ of $66.3\text{‰} \pm 1.7\text{‰}$. Plants from eastern North America and from the Ohio-Maryland region showed a larger fossil fuel influence with a mean $\Delta^{14}\text{C}$ of $58.8\text{‰} \pm 3.9\text{‰}$ and $55.2\text{‰} \pm 2.3\text{‰}$, respectively, corresponding to $2.7 \text{ ppm} \pm 1.5 \text{ ppm}$ and $4.3 \text{ ppm} \pm 1.0 \text{ ppm}$ of added fossil fuel CO₂ relative to the mountain west. A model–data comparison suggests that surveys of annual plant $\Delta^{14}\text{C}$ can provide a useful test of atmospheric mixing in transport models that are used to estimate the spatial distribution of carbon sources and sinks.

Citation: Hsueh, D. Y., N. Y. Krakauer, J. T. Randerson, X. Xu, S. E. Trumbore, and J. R. Southon (2007), Regional patterns of radiocarbon and fossil fuel-derived CO₂ in surface air across North America, *Geophys. Res. Lett.*, *34*, L02816, doi:10.1029/2006GL027032.

1. Introduction

[2] The radiocarbon (¹⁴C) produced by atomic weapons testing in the late 1950s and early 1960s has served as a powerful tracer of atmospheric and ocean transport, air-sea gas exchange, and the age distribution of carbon in terrestrial ecosystems. After reaching nearly 1000‰ in the northern hemisphere troposphere in 1963, $\Delta^{14}\text{C}$ levels have declined systematically as a result of dilution primarily from carbon exchange with ocean and terrestrial biosphere reservoirs [Nydal and Lovseth, 1983]. Key processes that regulate the contemporary distribution of atmospheric $\Delta^{14}\text{C}$ include rates of ocean mixing and air-sea gas exchange [Broecker *et al.*, 1985], carbon cycling within terrestrial ecosystems [Trumbore, 2000], cosmogenic production [Lingenfelter, 1963], re-entrainment of older stratospheric air in the troposphere [Hesshaimer and Levin, 2000], and fossil fuel emissions. At a regional scale, the relative importance of these processes varies. In the Southern Hemisphere, for example, upwelling and subduction of intermediate and deep water masses (with low $\Delta^{14}\text{C}$ levels) causes large latitudinal gradients, with a minimum in atmospheric $\Delta^{14}\text{C}$ over the Southern Ocean [Levin and

Hesshaimer, 2000]. In the Northern Hemisphere, large urban and industrial centers in North America, Europe, and Asia create plumes of fossil fuel-enriched CO₂ that are depleted in $\Delta^{14}\text{C}$ [Randerson *et al.*, 2002; Levin *et al.*, 2003; Turnbull *et al.*, 2006].

[3] The rate at which these fossil fuel plumes are lofted off the northern continents and mixed between the northern and southern hemispheres in atmospheric models critically determines the distribution and magnitude of carbon sources and sinks in ‘top down’ inversions that take advantage of atmospheric observations. Atmospheric models that trap too much fossil fuel CO₂ near the surface, for example, may require erroneously large carbon sinks to match surface observations [e.g., Gurney *et al.*, 2004]. Vertical mixing in atmospheric models is challenging to represent, in part because some of the key processes (including convection) occur at spatial resolutions smaller than the size of the average grid cell. Tracers that can serve as potential constraints on atmospheric mixing processes include water vapor, radon, and $\Delta^{14}\text{C}$. Past work using radon and $\Delta^{14}\text{C}$ provides evidence for strong regional and vertical gradients in fossil fuel CO₂ across Europe [Levin *et al.*, 2003]. $\Delta^{14}\text{C}$ is a particularly sensitive tracer of fossil fuel emissions in the contemporary (2006) atmosphere; 1 ppm of CO₂ added from fossil fuels causes a depletion of $\Delta^{14}\text{C}$ by approximately 2.8‰, which is near the precision of contemporary accelerator mass spectrometers [Turnbull *et al.*, 2006].

[4] In this study, we measured the $\Delta^{14}\text{C}$ of corn plants across North America during the summer of 2004. We had three objectives. First, we wanted to assess whether annual plants could be used to obtain time-integrated atmospheric samples over a period of several months, as a complement to ground and aircraft flask sampling approaches. Second, we wanted to better understand how fossil fuel emissions disperse over the continent. To what extent, for example, do the Rocky Mountains impede the surface flow of fossil fuel CO₂ from the west coast to the east coast? Third, by mapping regional variations in atmospheric $\Delta^{14}\text{C}$ we hoped to improve our ability to use $\Delta^{14}\text{C}$ as a tracer in ecosystem studies examining rapid turnover pools [e.g., Gaudinski *et al.*, 2001].

2. Materials and Methods

2.1. Sample Collection

[5] We collected samples of corn leaves (*Zea mays*) from North America during the summer of 2004. A few additional samples were collected from Venezuela, Brazil, and China. We relied on the generosity of colleagues to collect corn samples in places near where they lived or visited. Packets were sent to colleagues with a specific sampling

¹Department of Earth System Science, University of California, Irvine, California, USA.

²Division of Geological and Planetary Sciences, California Institute of Technology, Pasadena, California, USA.

Table 1. Regional Variability of $\Delta^{14}\text{C}$ and Fossil Fuel CO_2 Across North America

	Mountain West ^a	Eastern U.S. ^b	Ohio-Maryland ^c
Mean $\Delta^{14}\text{C}$, ‰	66.3 ± 1.7^d	58.8 ± 3.9	55.2 ± 2.3
Number of sites (n)	8	34	11
Change in $\Delta^{14}\text{C}$ relative to the Mountain West, ‰	-	-7.5 ± 4.3	-11.1 ± 2.9
Biosphere + ocean + stratosphere contribution, ^e ‰	-	0.0 ± 0.2	0.8 ± 0.3
Estimated $\Delta^{14}\text{C}$ change due to added fossil fuel CO_2 , ‰	-	-7.5 ± 4.3	-11.9 ± 2.9
Added fossil fuel CO_2 , ppm	-	2.7 ± 1.5	4.3 ± 1.0

^aIncludes all samples from Alberta, Idaho, Colorado, and New Mexico.

^bIncludes all samples from Nova Scotia, Massachusetts, New Hampshire, New York, Indiana, Ohio, Pennsylvania, Maryland, West Virginia, Kentucky, Tennessee, Virginia, Mississippi, Alabama, Georgia, and Florida.

^cIncludes all samples from Ohio, Pennsylvania, West Virginia, and Maryland.

^dError estimates for $\Delta^{14}\text{C}$ measurements were computed as the standard deviation of all individual site means within a given region.

^eError estimates for model-derived terrestrial biosphere, ocean, and stratosphere components are subjective and reflect combined uncertainties from atmospheric transport and surface fluxes. We conducted a sensitivity test of doubling and halving the residence times in the terrestrial biosphere, and report the results in the auxiliary material¹.

protocol, three paper coin envelopes for the samples, and a larger self-addressed envelope for sample return. To avoid sampling point sources such as highways or power plants, our protocol was to collect samples in remote locations. Specifically, we sampled more than 1.6 km away from highways, more than 45 meters from paved roads, and more than 20 meters away from houses or buildings that used natural gas or fossil fuels for heating. For the most part, we avoided sampling in major cities so that we could detect larger-scale regional patterns of $\Delta^{14}\text{C}$. At each site, cross-sections from three top leaves were collected, except in Hawaii and in Carlsbad, Clovis, and Riverside, California, where husks were sampled. In Alaska, an annual forb (*Matricaria matricariodes*) was substituted for corn because of the difficulty in locating corn in this region. Additional corn samples were also collected directly by the authors during July 17–23 from Alabama, Tennessee, Kentucky, Ohio, West Virginia, Pennsylvania, Maryland and Virginia. Most samples (45 out of 67) were collected in the field before the end of July.

2.2. Sample Preparation and Analysis

[6] Samples were dried at approximately 60–70°C for at least 48 hours, upon arrival at our laboratory. After drying, the plants were ground, and the bulk plant material (without any pretreatment) was converted to graphite using the process described by Santos *et al.* [2004]. Subsequently, the graphite was analyzed for $\Delta^{14}\text{C}$ using the W.M. Keck Carbon Cycle Accelerator Mass Spectrometer at UC Irvine. To ensure that we quantified the overall accuracy and to minimize the chance of differences due to running samples in different batches on the AMS, we included approximately 6 primary and 6 secondary standards with each wheel (along with 26 corn samples). We also made repeated measurements at 26 out of 67 sites to further establish continuity across the different AMS runs. Based on an analysis of our secondary standards, we concluded that the accuracy of any individual measurement was $\pm 2.3\%$. As a measure of precision, the pooled standard deviation across sites for which we made multiple measurements was 2.4%.

2.3. Estimating Fossil Fuel CO_2

[7] Ambient CO_2 that is assimilated by the corn (C_c , with units of ppm) consists of a background component

(C_{bg}) and local anomalies caused by terrestrial biosphere exchange (C_b), ocean exchange (C_o), and fossil fuel emissions (C_{ff}). Similarly, the $\Delta^{14}\text{C}$ of the components are Δ_c , Δ_{bg} , Δ_b , Δ_o , and Δ_{ff} . The mass balance equations are

$$C_c = C_{bg} + C_b + C_o + C_{ff} \quad (1)$$

$$\Delta_c * C_c \approx \Delta_{bg} * C_{bg} + \Delta_b * C_b + \Delta_o * C_o + \Delta_{ff} * C_{ff} \quad (2)$$

[8] We estimated background CO_2 levels (C_{bg}) using measurements from the NOAA Global Monitoring Division Niwot Ridge station. Niwot Ridge is a high elevation (3475 m.a.s.l.) continental site that is sampled during meteorological conditions representative of the free troposphere. Because most of the corn grew during May, June, and July of 2004, we constructed C_{bg} from the mean of observations during these three months. C_{bg} was equal to $378.4 \text{ ppm} \pm 2.7 \text{ ppm}$, based on an average and standard deviation of 41 flask samples. Δ_{bg} was assumed to equal the mean of the corn samples from the mountain west region (sample locations are given in the footnote of Table 1). Thus our estimates of C_{ff} were made relative to this clean air region defined by both CO_2 and $\Delta^{14}\text{C}$ measurements.

[9] Regional anomalies of C_b , C_o , Δ_b , and Δ_o , relative to Niwot Ridge, were taken from an analysis of atmospheric radiocarbon [Krakauer *et al.*, 2006] using the Model of Atmospheric Transport and Chemistry (MATCH) [Mahowald *et al.*, 1997]. MATCH was run with 26 vertical levels, a horizontal resolution of 5.5° , and with meteorological fields from the NCAR Community Climate Model v3 [Olsen and Randerson, 2004].

[10] We modeled fossil fuel releases in MATCH using the map from Andres *et al.* [1996] for 1995 emissions, scaled uniformly based on the Carbon Dioxide Information Analysis Center time series of global fossil emissions [Marland *et al.*, 2005] to account for the overall increase in emission levels between 1995 and 2004. The fossil emissions had a $1^\circ \times 1^\circ$ resolution that was aggregated to the resolution of our transport model.

¹Auxiliary material data sets are available at <ftp://ftp.agu.org/apend/gl/2006gl027032>. Other auxiliary material files are in the HTML.

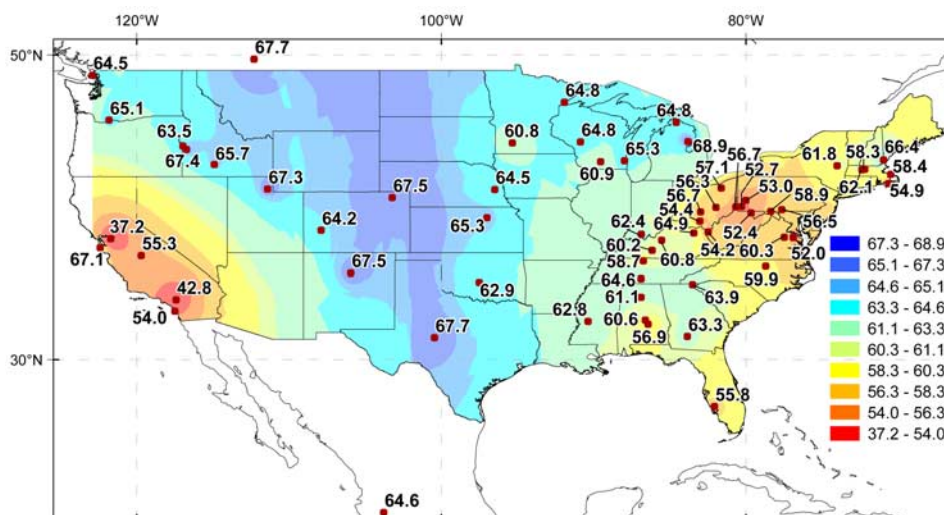


Figure 1. $\Delta^{14}\text{C}$ measurements of corn (*Zea mays*) across North America during the summer of 2004 (in units of ‰). During this period, a decrease of 2.8‰ corresponded to approximately 1 ppm of added fossil fuel CO_2 . The background color interpolation was generated using a spline fit based on 15 nearest neighbors with the Geostatistical Analyst tool in ESRI's ArcMap software.

[11] To model atmospheric $\Delta^{14}\text{C}$ gradients from terrestrial biosphere and ocean exchange, we generated regional Green's functions from our transport model. Our Green's functions corresponded to tracer releases over the 22 TransCom regions [Gurney *et al.*, 2004]. The tracer release was constant during each month of the year, allowing us to accurately represent seasonally varying fluxes. The spatial pattern of tracer release within each of the 11 terrestrial regions corresponded to the distribution of NPP predicted by CASA, while tracer release was spatially uniform within the 11 ocean regions. The $\Delta^{14}\text{C}$ of heterotrophic respiration within each terrestrial region was estimated using pulse-response functions from the Carnegie-Ames-Stanford Approach (CASA) biogeochemical model [Thompson and Randerson, 1999] convolved with the history of atmospheric $\Delta^{14}\text{C}$, based on tree ring records [Stuiver and Quay, 1981] and, since the 1950s, on atmospheric measurements [Levin and Kromer, 2004]. This meant that for temperate North America, the heterotrophic respiration flux had the same $\Delta^{14}\text{C}$ level entering into each tracer model grid cell within the region (a mean of 99.8‰), but the magnitude of this flux was distributed heterogeneously across the continent according to the CASA-derived pattern of NPP (that is equivalent to the pattern of heterotrophic respiration for this purpose). We used sea-surface $\Delta^{14}\text{C}$ derived from a simulation of bomb radiocarbon uptake with an ocean transport model [Krakauer *et al.*, 2006] and assumed an air-sea gas transfer velocity proportional to the square of wind speed [Dutay *et al.*, 2002] to estimate the spatial pattern of ocean ^{14}C uptake, and with the same set of pulse functions simulated the impact of ocean uptake of ^{14}C on atmospheric $\Delta^{14}\text{C}$.

[12] The model simulations also included stratosphere-troposphere exchange effects on regional patterns of CO_2 and $\Delta^{14}\text{C}$, but across North America, these effects were small (varying by less than 0.3‰). We did this by constructing pulse functions for northern, southern, and

equatorial tracer release in the stratosphere (at the 90 mb pressure level) and in the upper troposphere (at 200 mb) to allow us to simulate the effect of cosmogenic ^{14}C production in the upper atmosphere on atmospheric $\Delta^{14}\text{C}$ gradients near the surface.¹

3. Results

3.1. Observed Spatial Patterns

[13] In places with elevated levels of CO_2 from recently added fossil fuel emissions, $\Delta^{14}\text{C}$ levels were reduced (Figure 1). We found a decrease of $7.5\text{‰} \pm 4.3\text{‰}$ between the western mountain region of North America and eastern North America (Table 1). This corresponded to a 2.7 ± 1.5 ppm increase in fossil fuel CO_2 levels in the east, relative to the west. An even larger $\Delta^{14}\text{C}$ decrease of $11.1\text{‰} \pm 2.9\text{‰}$ was found between the western mountain region and the Ohio-Maryland region (including Ohio, Pennsylvania, West Virginia, and Maryland), corresponding to 4.3 ± 1.0 ppm of added fossil CO_2 . Sample locations, individual site $\Delta^{14}\text{C}$ measurements, and more detailed information about our measurement errors are provided in an auxiliary table.¹

[14] Near urban areas, $\Delta^{14}\text{C}$ gradients were even larger. In northern California, for example, $\Delta^{14}\text{C}$ at a coastal site (San Gregorio) was $67.1\text{‰} \pm 2.3\text{‰}$, whereas $\Delta^{14}\text{C}$ at a site ~ 95 km to the east and north (Brentwood) was $37.2\text{‰} \pm 2.3\text{‰}$. The 30‰ decrease at Brentwood, relative to the coast, corresponded to 10.9 ppm of locally-added fossil fuel CO_2 that probably originated from cities in the San Francisco Bay Area. Low $\Delta^{14}\text{C}$ was also observed near Clovis, CA ($55.3\text{‰} \pm 2.3\text{‰}$) and Riverside, CA ($42.8\text{‰} \pm 2.3\text{‰}$).

[15] Comparison with nearby flask observations showed that the annual plants provided an integrated measure of atmospheric $\Delta^{14}\text{C}$ during the time of their growth. The mean of annual plants collected from the western mountain

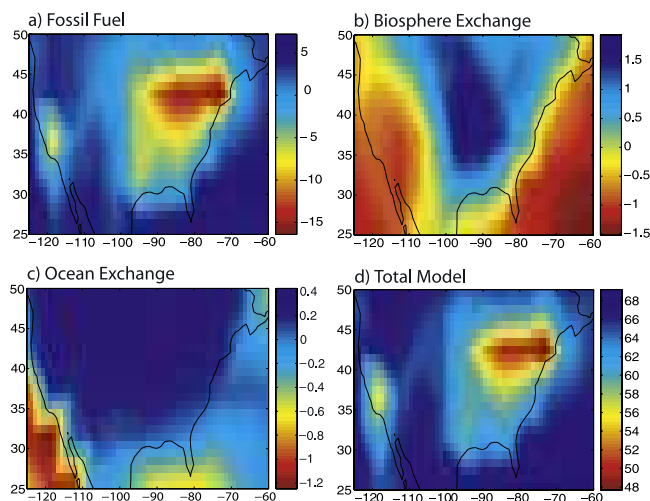


Figure 2. Contributions to surface atmospheric $\Delta^{14}\text{C}$ anomalies (with units of ‰) caused by (a) fossil fuel emissions, (b) terrestrial biosphere exchange, and (c) ocean exchange as derived from a global model during May–July of 2004 and (d) the combined influence of these processes, along with the effects of stratosphere-troposphere mixing. The background $\Delta^{14}\text{C}$ in Figure 2d was adjusted by a single uniform scalar so that the mean of the model was the same as the mean of observations from the western mountain region (defined in Table 1). The MATCH model was used in these simulations with fluxes described in the text. Panels shown here were interpolated from the original model resolution of approximately 5.5° . Stratosphere-troposphere exchange (data not shown) contributed to a small enrichment of surface $\Delta^{14}\text{C}$ across the western mountains (less than 0.3‰) as compared with other regions closer to sea level.

region ($66.3\text{‰} \pm 1.7\text{‰}$) was the same, within measurement error, as the mean of $\Delta^{14}\text{C}$ measured by flasks during May, June, and July at Niwot Ridge ($64.4\text{‰} \pm 3.3\text{‰}$, $n = 12$) as reported by *Turnbull et al.* [2006]. An independent set of 8 flasks collected from Niwot Ridge during April, June, and July of 2004 (extracted and measured at UC Irvine) yielded a similar mean of $67.6\text{‰} \pm 3.0\text{‰}$. Annual plants sampled near Healy in interior Alaska ($65.2\text{‰} \pm 2.3\text{‰}$) were similar to flask measurements collected at the same location in June and August ($65.6\text{‰} \pm 7.5\text{‰}$, $n = 4$ (E.A.G. Schuur, unpublished data, 2004)).

3.2. Model-Data Comparison

[16] The dominant driver of regional variation in $\Delta^{14}\text{C}$ across North America as predicted by our model was fossil fuel emissions (Figure 2). Fossil fuel emissions created two local minima of $\Delta^{14}\text{C}$ across the continent. One was located over California (Figure 2a). The other was stronger and was located over the northeastern U.S. between 40°N and 45°N and 70°W and 90°W . Respiration of bomb ^{14}C from terrestrial ecosystems caused greater enrichment of surface air in the east (where respiration fluxes were stronger) and thus partly offset the depletion of $\Delta^{14}\text{C}$ in this region caused by fossil fuels (Figure 2b). Terrestrial ecosystem respiration caused a maximum in surface air $\Delta^{14}\text{C}$ across

the Midwest (Oklahoma, Nebraska, and North and South Dakota). Thus, even though respiration rates were higher in the temperate forests to the east (which would enrich surface CO_2 in $\Delta^{14}\text{C}$), it is likely that longer residence times of surface air in the middle of the continent, including entrainment of air from Canada, contributed to the $\Delta^{14}\text{C}$ maximum located there. Ocean exchange contributed only minimally to continental patterns across North America (Figure 2c), although this flux induced variations in excess of 1‰ near coastal zones.

[17] Overall the model captured some but not the entire pattern of observed $\Delta^{14}\text{C}$, perhaps in part because of its coarse spatial resolution and from information loss caused by our use of uniform monthly-mean Green's functions. Between the eastern U.S. region and the mountain west region defined in Table 1, model-predicted $\Delta^{14}\text{C}$ differences from fossil fuel, terrestrial biosphere, ocean, and cosmogenic production processes were -8.5‰ , $+0.4\text{‰}$, -0.3‰ , and -0.1‰ , respectively. Combined, the difference predicted by the model of -8.5‰ was approximately the same as the observed difference of $-7.5\text{‰} \pm 2.9\text{‰}$. Model-predicted differences between the Ohio-Maryland region and the mountain west region were -13.9‰ , $+0.9\text{‰}$, 0.0‰ , and -0.1‰ , and again, the combined model difference of -13.1‰ was similar to the observed difference of $-11.1\text{‰} \pm 2.9\text{‰}$.

4. Discussion

4.1. Understanding the Movement of Fossil Fuel-Derived CO_2

[18] *Turnbull et al.* [2006] demonstrate that ^{14}C has several advantages over CO or SF_6 as a tracer of local sources of fossil fuel-derived CO_2 . Both *Turnbull et al.* [2006] and *Potosnak et al.* [1999] show that air within the planetary boundary layer over New England during summer has between 0.5 and 5 ppm of CO_2 added from nearby fossil fuel emissions. Our analysis provides additional support for a local fossil fuel source of over rural parts of New England and shows that elevated levels of CO_2 from fossil fuel emissions existed across most of the eastern U.S. during the summer of 2004 (with a mean of $2.7 \text{ ppm} \pm 1.5 \text{ ppm}$). Similar levels of fossil fuel CO_2 have been reported for remote parts of Europe, including at the Schauinsland station in Germany [*Levin and Kromer*, 1997]. Near cities, our analysis shows that fossil fuel-derived CO_2 can be an order of magnitude larger than in nearby rural environments. This finding is consistent with continuous CO_2 and $\delta^{13}\text{C}$ measurements reported from Salt Lake City, Utah [*Pataki et al.*, 2003] and $\Delta^{14}\text{C}$ measurements from Heidelberg, Germany [*Levin et al.*, 2003].

[19] The high $\Delta^{14}\text{C}$ values observed across the mountain west imply that fossil fuel emissions from California and other western coastal states are either substantially diluted or lofted off the surface by the time they reach this region or that these emissions leave the continent via another route (e.g., entrainment into a southerly flow around the Pacific high that forms during summer). If the latter is correct, our work suggests that atmospheric sampling strategies designed to measure North American continental outflow [*Wofsy and Harriss*, 2002] must sample southern as well as eastern borders.

4.2. Strengths and Weaknesses of Sampling *Zea Mays*

[20] The design of an atmospheric sampling program based on annual plants has advantages and disadvantages. Compared to tree rings, annual plants have the advantage that all of the biomass accumulates during a single growing season. This removes the complication of having to estimate the contribution of multi-year starch reserves to the current year's biomass increment. In boreal forest ecosystems, temporal offsets between gross primary production and bole increment suggest these starch inputs may be substantial [Rocha *et al.*, 2006]. On the other hand, annual plants decompose quickly, so it is challenging to develop time series that extend back more than a few years.

[21] As compared with flasks, annual plants provide an efficient means to capture time-integrated atmospheric $\Delta^{14}\text{C}$ samples over a period of weeks to months. This offers a unique advantage in terms of rapidly mapping large-scale environmental gradients in both rural and urban settings in a cost-effective manner. Also, the time-integrated samples are particularly valuable for assessing seasonal and annual carbon sources. Possible future applications include testing for leaks from subterranean CO_2 sequestration projects, and where CO/CO_2 emissions ratios are known, monitoring of atmospheric CO concentrations near industrial sources. Annual plants also provide a unique test of the combined effect of fossil fuel emissions, boundary layer mixing, and atmospheric transport in mesoscale and global atmospheric models used to study the global carbon cycle. Models that trap too much fossil fuel over continental areas will predict regional decreases in $\Delta^{14}\text{C}$ that are larger than observations. A disadvantage of using annual plants is that the exact timing of plant carbon fixation diurnally and on synoptic timescales is difficult to quantify without investment in other measurement approaches.

[22] The biomass of the C_4 and C_3 annual plants measured here represents a time-integrated $\Delta^{14}\text{C}$ value during the day, weighted by factors that control rates of photosynthesis. As a result, our samples measure atmospheric $\Delta^{14}\text{C}$ levels during periods when the planetary boundary layer was well developed. This diurnal sampling pattern differs substantially from that obtained when canisters with pinhole valves or constant speed pumps are used to collect integrated air samples over a period of days to weeks. These latter sampling approaches capture CO_2 in proportion to its atmospheric abundance and thus have the tendency to weight nighttime periods more heavily than daytime periods. These differences in sampling protocol have the potential to influence model-data comparisons, and need to be considered in future studies that use annual plant $\Delta^{14}\text{C}$ measurements to quantitatively assess model transport.

5. Conclusions

[23] Our measurements provide evidence of large coherent variations in atmospheric $\Delta^{14}\text{C}$ across the North American continent in excess of 10‰ and of even larger magnitude near urban areas. The highest levels of $\Delta^{14}\text{C}$ (and the lowest levels of fossil fuel-derived CO_2) were observed across the mountain west. The clean air in this region implies that fossil fuel-enriched surface air from the west coast is either substantially diluted or lofted off the

surface before reaching the Rocky Mountains, or that it leaves the continent via a separate route. The spatial pattern derived from the observations and model simulations identify fossil fuel emissions as the major driver of regional variability across the continent, with a small contribution from terrestrial biosphere exchange. This analysis, along with other recent work [Levin *et al.*, 2003; Turnbull *et al.*, 2006], implies that a comprehensive survey of $\Delta^{14}\text{C}$ would serve as a strong constraint on vertical transport and mixing of fossil fuel plumes in mesoscale and global atmospheric models. Important next steps include extending this analysis to Europe, Asia, and South America, and to combine these measurements with aircraft data and higher resolution models to examine inflow and outflow patterns of air over North America.

[24] Over the next few decades, fossil emissions are expected to increase and as a consequence, the regional gradients of $\Delta^{14}\text{C}$ shown in Figure 1 are likely to strengthen. Simultaneously, the rate of decline of atmospheric $\Delta^{14}\text{C}$ is expected to remain about the same as ^{14}C uptake by the oceans slows [Caldeira *et al.*, 1998]. Combined, these two effects will make it increasingly critical for ecosystem ecologists to quantify local atmospheric $\Delta^{14}\text{C}$ in studies that use radiocarbon as a tracer of rapidly exchanging pools.

[25] **Acknowledgments.** We gratefully acknowledge support from NSF EAR-0402062 and NASA NNG05GD126. We thank the following people for collecting samples: J. E. Anderson, D. Baldocchi, J. C. Beckwith, T. Berggren, J. Chanton, and M. Coakely, G. J. Collatz, M. Conte, P. S. Curtis, K. Dutta, J. Ehleringer, J. Fessenden, L. Flanagan, N. Goulden, J. Harden, S. Hobbie, A. Hoffman, D. Hollinger, R. A. Houghton, J. Hughes Martiny, P. Kasibhatla, J. Y. King, C. T. Lai, D. LeBauer, H. Liu, D. H. Loyd Jr., Y. Luo, L. Masiello, J. E. Munger, J. W. Munger, D. Nowinski, J. Okeefe, T. Perez, A. Rocha, D. R. Sandquist, T. Schimel, T. Schuur, C. Scott, C. Still, A. Trumbore, S. B. Verma, C. Vogel, G. Welp, and L. Ziolkowski. We thank G. dos Santos for advice on laboratory analysis, A. V. Rocha for assistance with fieldwork, S. M. Cheong for assistance with figure design, and J. Miller and S. Lehman for sharing CO_2 and $\Delta^{14}\text{C}$ data from Niwot Ridge.

References

- Andres, R. J., G. Marland, I. Fung, and E. Matthews (1996), A $1^\circ \times 1^\circ$ distribution of carbon dioxide emissions from fossil fuel consumption and cement manufacture, 1950–1990, *Global Biogeochem. Cycles*, *10*, 419–430.
- Broecker, W.S., T.-H. Peng, G. Ostlund, and M. Stuiver (1985), The distribution of bomb radiocarbon in the ocean, *J. Geophys. Res.*, *90*, 6953–6970.
- Caldeira, K., G. H. Rau, and P. B. Duffy (1998), Predicted net efflux of radiocarbon from the ocean and increase in atmospheric radiocarbon content, *Geophys. Res. Lett.*, *25*, 3811–3814.
- Dutay, J. C., et al. (2002), Evaluation of ocean model ventilation with CFC-11: Comparison of 13 global ocean models, *Ocean Modell.*, *4*, 89–120.
- Gaudinski, J. B., et al. (2001), The age of fine-root carbon in three forests of the eastern United States measured by radiocarbon, *Oecologia*, *129*, 420–429.
- Gurney, K. R., et al. (2004), Transcom 3 inversion intercomparison: Model mean results for the estimation of seasonal carbon sources and sinks, *Global Biogeochem. Cycles*, *18*, GB1010, doi:10.1029/2003GB002111.
- Hesshaimer, V., and I. Levin (2000), Revision of the stratospheric bomb $^{14}\text{CO}_2$ inventory, *J. Geophys. Res.*, *105*, 11,641–11,658.
- Krakauer, N. Y., et al. (2006), Carbon isotope evidence for the latitudinal distribution and wind speed dependence of the air-sea gas transfer velocity, *Tellus, Ser. B*, *58*, 390–417.
- Levin, I., and V. Hesshaimer (2000), Radiocarbon—A unique tracer of global carbon cycle dynamics, *Radiocarbon*, *42*, 69–80.
- Levin, I., and B. Kromer (1997), Twenty years of atmospheric $^{14}\text{CO}_2$ observations at Schauinsland station, Germany, *Radiocarbon*, *39*, 205–218.

- Levin, I., and B. Kromer (2004), The tropospheric $^{14}\text{CO}_2$ level in mid-latitudes of the Northern Hemisphere (1959–2003), *Radiocarbon*, *46*, 1261–1272.
- Levin, I., B. Kromer, M. Schmidt, and H. Sartorius (2003), A novel approach for independent budgeting of fossil fuel CO_2 over Europe by $^{14}\text{CO}_2$ observations, *Geophys. Res. Lett.*, *30*(23), 2194, doi:10.1029/2003GL018477.
- Lingenfelter, R. E. (1963), Production of carbon 14 by cosmic-ray neutrons, *Rev. Geophys.*, *1*, 35–55.
- Mahowald, N. M., P. J. Rasch, B. E. Eaton, S. Whittlestone, and R. G. Prinn (1997), Transport of $^{222}\text{radon}$ to the remote troposphere using the Model of Atmospheric Transport and Chemistry and assimilated winds from ECMWF and the National Center for Environmental Prediction/NCAR, *J. Geophys. Res.*, *102*(D23), 28,139–28,152.
- Marland, G., et al. (2006), Global, regional, and national fossil fuel CO_2 emissions, Carbon Dioxide Inf. Anal. Cent., Oak Ridge Natl. Lab., U. S. Dep. of Energy, Oak Ridge, Tenn.
- Nydal, R., and K. Lovseth (1983), Tracing bomb ^{14}C in the atmosphere 1962–1980, *J. Geophys. Res.*, *88*, 3621–3642.
- Olsen, S. C., and J. T. Randerson (2004), Differences between surface and column atmospheric CO_2 and implications for carbon cycle research, *J. Geophys. Res.*, *109*, D02301, doi:10.1029/2003JD003968.
- Pataki, D. E., D. R. Bowling, and J. R. Ehleringer (2003), Seasonal cycle of carbon dioxide and its isotopic composition in an urban atmosphere: Anthropogenic and biogenic effects, *J. Geophys. Res.*, *108*(D23), 4735, doi:10.1029/2003JD003865.
- Potosnak, M. J., S. C. Wofsy, A. S. Denning, T. J. Conway, J. W. Munger, and D. H. Barnes (1999), Influence of biotic exchange and combustion sources on atmospheric CO_2 concentrations in New England from observations at a forest flux tower, *J. Geophys. Res.*, *104*, 9561–9570.
- Randerson, J. T., I. G. Enting, E. A. G. Schuur, K. Caldeira, and I. Y. Fung (2002), Seasonal and latitudinal variability of troposphere $\Delta^{14}\text{CO}_2$: Post bomb contributions from fossil fuels, oceans, the stratosphere, and the terrestrial biosphere, *Global Biogeochem. Cycles*, *16*(4), 1112, doi:10.1029/2002GB001876.
- Rocha, A. V., et al. (2006), On linking interannual tree ring variability with observations of whole-forest CO_2 flux, *Global Change Biol.*, *8*, 1378–1389.
- Santos, G. M., et al. (2004), Magnesium perchlorate as an alternative water trap in AMS graphite sample preparation: A report on sample preparation at KCCAMS at the Univ. of California, Irvine, *Radiocarbon*, *46*, 165–173.
- Stuiver, M., and P. D. Quay (1981), Atmospheric ^{14}C changes resulting from fossil-fuel CO_2 release and cosmic-ray flux variability, *Earth Planet. Sci. Lett.*, *53*, 349–362.
- Thompson, M. V., and J. T. Randerson (1999), Impulse response functions of terrestrial carbon cycle models: method and application, *Global Change Biol.*, *5*, 371–394.
- Trumbore, S. (2000), Age of soil organic matter and soil respiration: Radiocarbon constraints on belowground C dynamics, *Ecol. Appl.*, *10*, 399–411.
- Turnbull, J. C., J. B. Miller, S. J. Lehman, P. P. Tans, R. J. Sparks, and J. Southon (2006), Comparison of $^{14}\text{CO}_2$, CO , and SF_6 as tracers for recently added fossil fuel CO_2 in the atmosphere and implications for biological CO_2 exchange, *Geophys. Res. Lett.*, *33*, L01817, doi:10.1029/2005GL024213.
- Wofsy, S. C., and R. C. Harriss (2002), The North American Carbon Program (NACP), 56 pp., U. S. Global Change Res. Program, Washington, D. C.

D. Y. Hsueh, J. T. Randerson, J. R. Southon, S. E. Trumbore, and X. Xu, Department of Earth System Science, University of California, Croul Hall, Irvine, CA 92697, USA. (dhsueh@uci.edu; jranders@uci.edu; jsouthon@uci.edu; setrumbo@uci.edu; xxu@uci.edu)

N. Y. Krakauer, Division of Geological and Planetary Sciences, California Institute of Technology, 1200 E. California Ave., Pasadena, CA 91125, USA. (niryk@caltech.edu)